Biophysical Journal
Correction

Biophysical Society

Quantifying single-cell diacylglycerol signaling kinetics after uncaging

David T. Gonzales, Milena Schuhmacher, H. Mathilda Lennartz, Juan M. Iglesias-Artola, Sascha M. Kuhn, Pavel Barahtjan, Christoph Zechner,* and Andre Nadler*

(Biophysical Journal *122*, 4699–4709; December 19, 2023)

In the originally published version of this article, in Figure 3B, the example image of SAG-loaded cells was mistakenly shown also for SOG. The figure has been replaced by a corrected version. The authors are grateful to Prof. Dr. John Sondek for pointing this out.

The authors further noticed a mistake in the calculation of the likelihood threshold used to determine approximate 95% confidence intervals from profile likelihoods. Simultaneous confidence regions for parameter x at confidence level α are approximated from a profile likelihood $PL(x)$ as $\left\{x \middle| PL(x) < \left(-l(\hat{x}) + \chi^2(\alpha, df)/2\right)\right\}$, with $l(\hat{x})$ as the log-likelihood function evaluated at the maximum likelihood parameter $\hat{x}$ and $\chi^2(\alpha, df)$ as the α-quantile of the χ^2-distribution with df degrees of freedom, which is set to the number of unknown model parameters.

In our previous analysis, the factor of $1/2$ in front of $\chi^2(\alpha, df)$ was omitted, and df was incorrectly set to (*number of parameters*) $-$ 1 in the code. Effectively, this caused the likelihood thresholds to be too large, leading to an overestimation of the 95% confidence intervals. The authors note that the optimal parameter estimates themselves are not affected by this mistake. After correcting, the confidence intervals became narrower, such that all conclusions of the manuscript remain entirely supported. Figures 2 and 5 in the main text and Tables S1–S4, Figures S1–S4 and S6–S14, and the text in the Supporting material were updated to reflect these changes. The Edmond repository was updated with the corrected code.

The paper contains additional typographic and production errors related to citations of sections and figures in the Supporting material. First, the last sentence of the first paragraph on page 4704 should read as follows: "Loading concentrations were adjusted to achieve comparable incorporation levels for all cgDAGs (Fig. S23)." Second, the fifth sentence of the second paragraph on page 4704 should read as follows: "The data were manually curated by removing traces from apoptotic cells and cells that moved too much during the acquisition (see Supporting material for details on uncaging experiments and image analysis)." Third, the ninth sentence in the "Inference of rate parameters and photoreaction yields from single-cell time trace data" section on page 4705 should read as follows: "Representative inference results for SAG are shown in Fig.5, *A–C* (see Figures S6–S12 of the Supporting material for the remaining DAG species)." Fourth, in the second paragraph of the Discussion, the sentence that begins with "This is remarkable because…" was mistakenly repeated. The correct text of that paragraph is as follows:

"Directly measuring single-cell uncaging photoreaction yields is not possible using our previously published methodology, which requires separate experiments for photoreaction yield determination and acquisition of time-trace data. To address this, we treated the initial photoreaction yield as an additional parameter that is inferred simultaneously with other parameters such as lipid-protein affinities and rates for *trans*-bilayer movement and turnover. We find that the resulting model can still be fully parameterized from time-trace data if the data quality is sufficient. This is remarkable because our previous population-level analysis required the acquisition of dose-response curves via uncaging light titrations to uniquely identify all model parameters. This seems to be the case as our current approach exploits natural protein-level variations to sample the concentration space. The main determinant of parameter identifiability was found to be measurement noise. The number

*Correspondence: zechner@mpi-cbg.de or nadler@mpi-cbg.de

https://doi.org/10.1016/j.bpj.2024.03.031

of cell traces used can also improve parameter identifiability but results in more computational effort, and improvements begin to diminish after a certain number of cells ($n = \sim 100$). This suggests that improvements in imaging technology and image analysis pipelines will directly result in improved capability for extracting quantitative parameters from live-cell time-trace data."

Finally, the first sentence in section S5 of the Supporting material should have read as follows: "Model parameters and parameter identifiability were estimated by MLE and profile likelihoods for each DAG species using all cells in the population individually as described in S1 using the model without k_{out}."

The authors sincerely apologize for having missed these mistakes before publication.

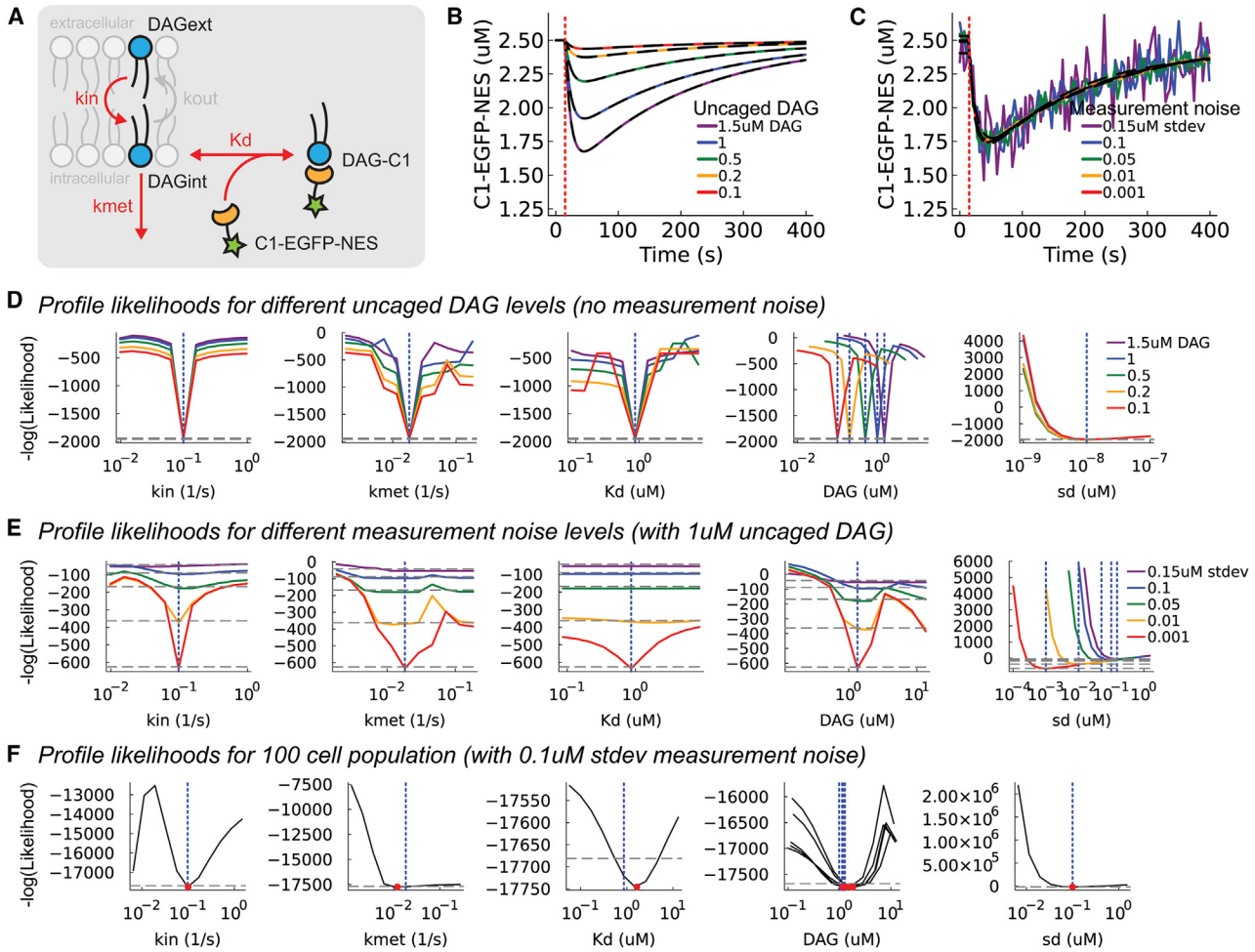

Figure 2. Approach and testing of parameter identifiability in a model of signaling lipid dynamics using simulated data. (*A*) Schematic of a model for signaling lipid dynamics. DAG at the outer leaflet of the cell membrane (DAG_{ext}) can flip into the inner leaflet (DAG_{int}), where it can either be metabolized or recruit C1-EGFP-NES proteins in the cytosol to for the membrane-associated complex DAG-C1. Rate parameters (k_{in}, k_{met}, K_d) of the model are shown in red. Simulated single-cell traces of C1-EGFP-NES at (*B*) different uncaged DAG concentrations (0.1, 0.25, 0.5, 1.0, and 2.0 μM) and no measurement noise and (*C*) different levels of measurement noise (0.001, 0.01, 0.05, 0.1, and 0.15 μM) and fixed uncaged DAG at 1.5 μM. Fits of each individual cell are shown in black dashed lines. Red vertical dotted line indicates the time of ultraviolet exposure that results in DAG uncaging. Profile likelihoods of the model parameters from each individual cell at different uncaged DAG concentrations and levels of measurement noise are shown in (*D*) and (*E*), respectively. (*F*) Profile likelihoods of the model parameters using data from traces of 100 cells with a fixed measurement noise of 0.1 μM. Profile likelihoods of uncaged DAG are shown for five representative cells only. For all profile likelihood plots, gray horizontal dashed lines indicate the 95% likelihood-based confidence interval threshold, blue vertical dotted lines indicate the true value of the parameter, and red circles indicate the maximum likelihood estimation of the parameter. True parameter values for the model are $k_{in} = 0.098\ s^{-1}$, $k_{met} = 0.01823\ s^{-1}$, and $K_d = 0.866\ \mu$M. The parameter SD is an additional fitting parameter that represents the standard deviation of the measurement noise. To see this figure in color, go online. (corrected)

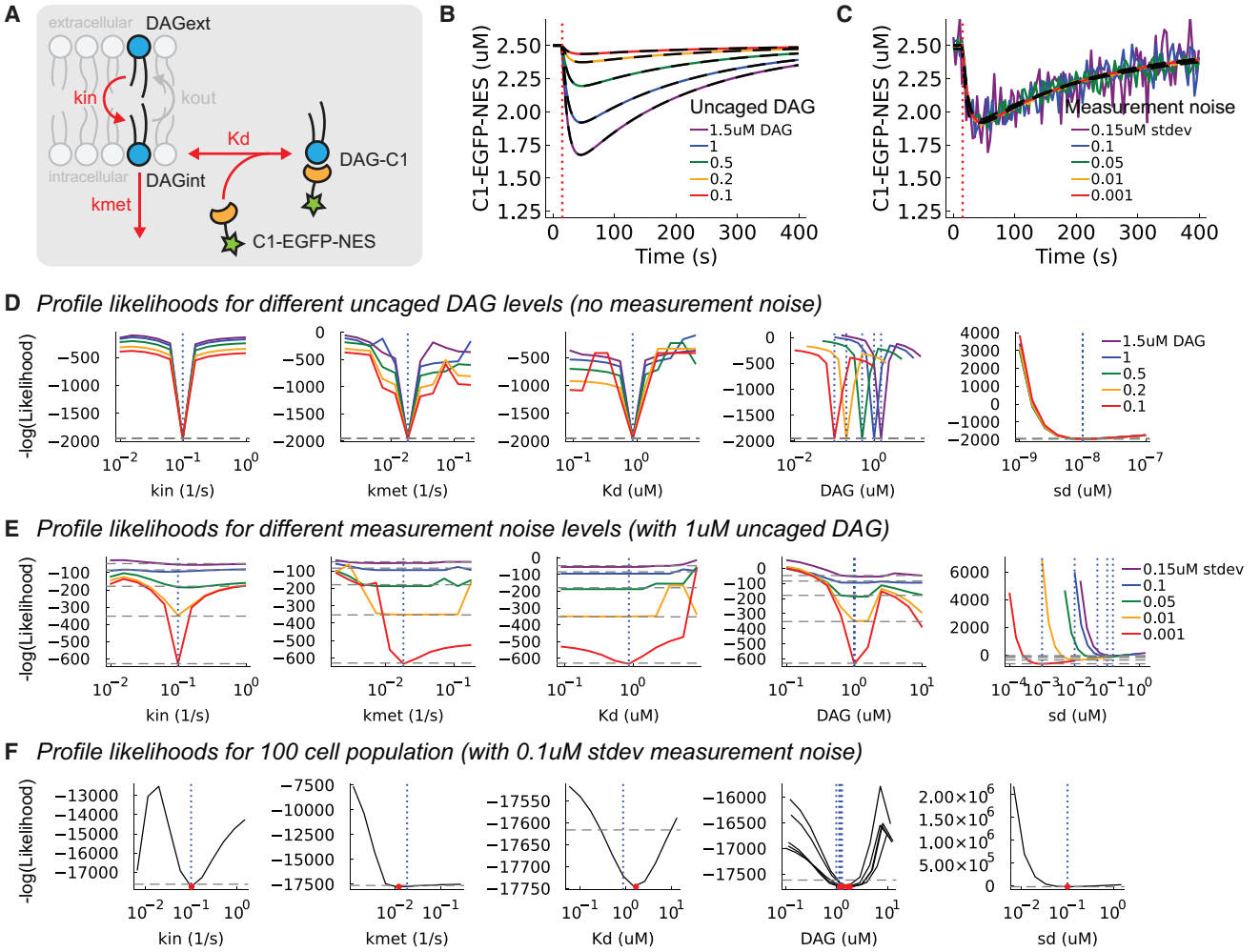

Figure 2. Approach and testing of parameter identifiability in a model of signaling lipid dynamics using simulated data. (*A*) Schematic of a model for signaling lipid dynamics. DAG at the outer leaflet of the cell membrane (DAG_{ext}) can flip into the inner leaflet (DAG_{int}), where it can either be metabolized or recruit C1-EGFP-NES proteins in the cytosol to for the membrane-associated complex DAG-C1. Rate parameters (k_{in}, k_{met}, K_d) of the model are shown in red. Simulated single-cell traces of C1-EGFP-NES at (*B*) different uncaged DAG concentrations (0.1, 0.25, 0.5, 1.0, and 2.0 μM) and no measurement noise and (*C*) different levels of measurement noise (0.001, 0.01, 0.05, 0.1, and 0.15 μM) and fixed uncaged DAG at 1.5 μM. Fits of each individual cell are shown in black dashed lines. Red vertical dotted line indicates the time of ultraviolet exposure that results in DAG uncaging. Profile likelihoods of the model parameters from each individual cell at different uncaged DAG concentrations and levels of measurement noise are shown in (*D*) and (*E*), respectively. (*F*) Profile likelihoods of the model parameters using data from traces of 100 cells with a fixed measurement noise of 0.1 μM. Profile likelihoods of uncaged DAG are shown for five representative cells only. For all profile likelihood plots, gray horizontal dashed lines indicate the 95% likelihood-based confidence interval threshold, blue vertical dotted lines indicate the true value of the parameter, and red circles indicate the maximum likelihood estimation of the parameter. True parameter values for the model are $k_{in} = 0.098\ s^{-1}$, $k_{met} = 0.01823\ s^{-1}$, and $K_d = 0.866\ \mu M$. The parameter SD is an additional fitting parameter that represents the standard deviation of the measurement noise. To see this figure in color, go online. (original)

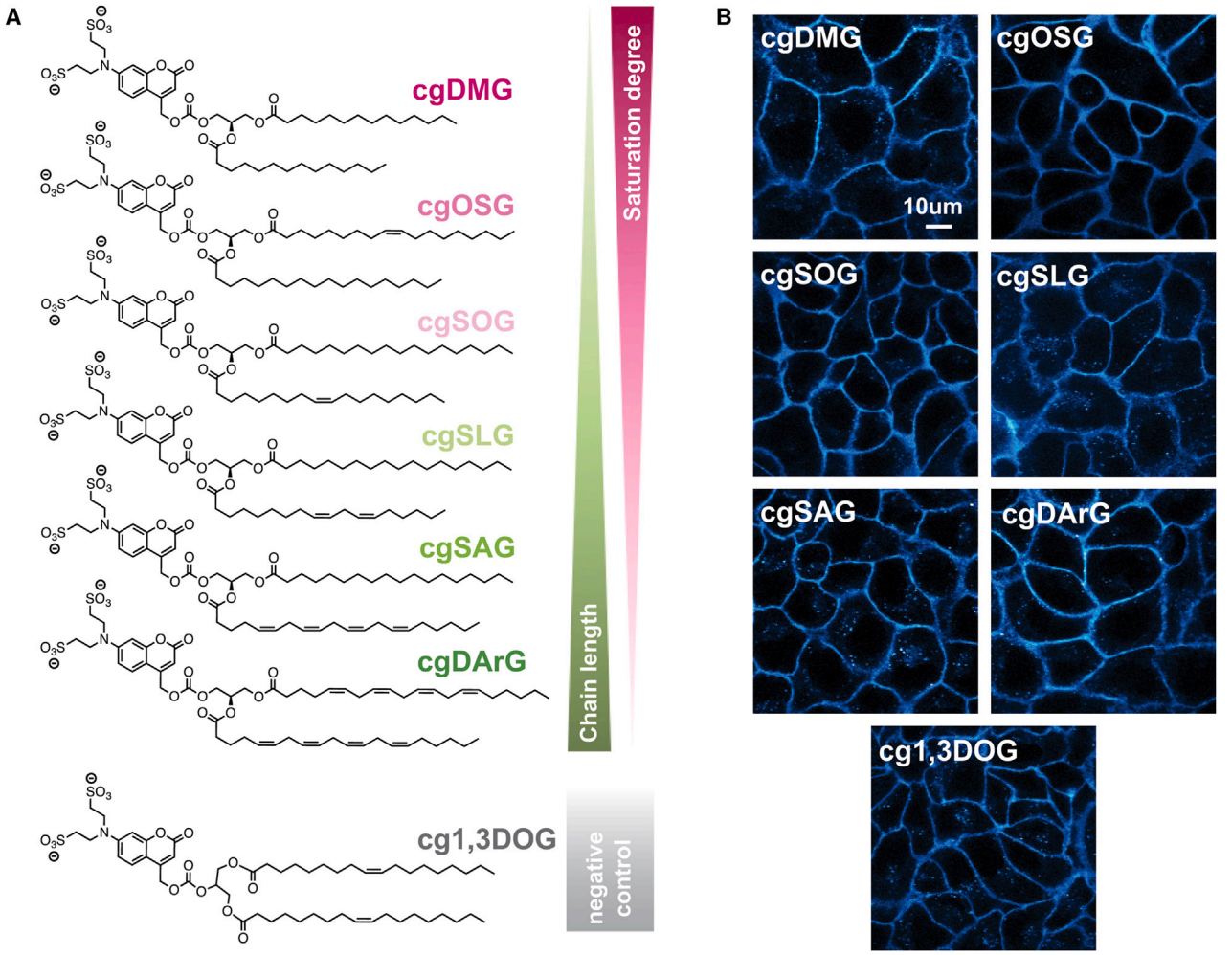

Figure 3. Chemistry of DAGs. (*A*) Chemical structures of the different DAGs used in this study sorted by increasing saturation degree (*top to bottom*). 1,3-Dioleoylglycerol does not recruit the C1-containing effector protein and is used as a negative control. (*B*) Confocal fluorescence microscopy of HeLa Kyoto cells with cgDAGs localizing in the plasma membrane. To see this figure in color, go online. (corrected)

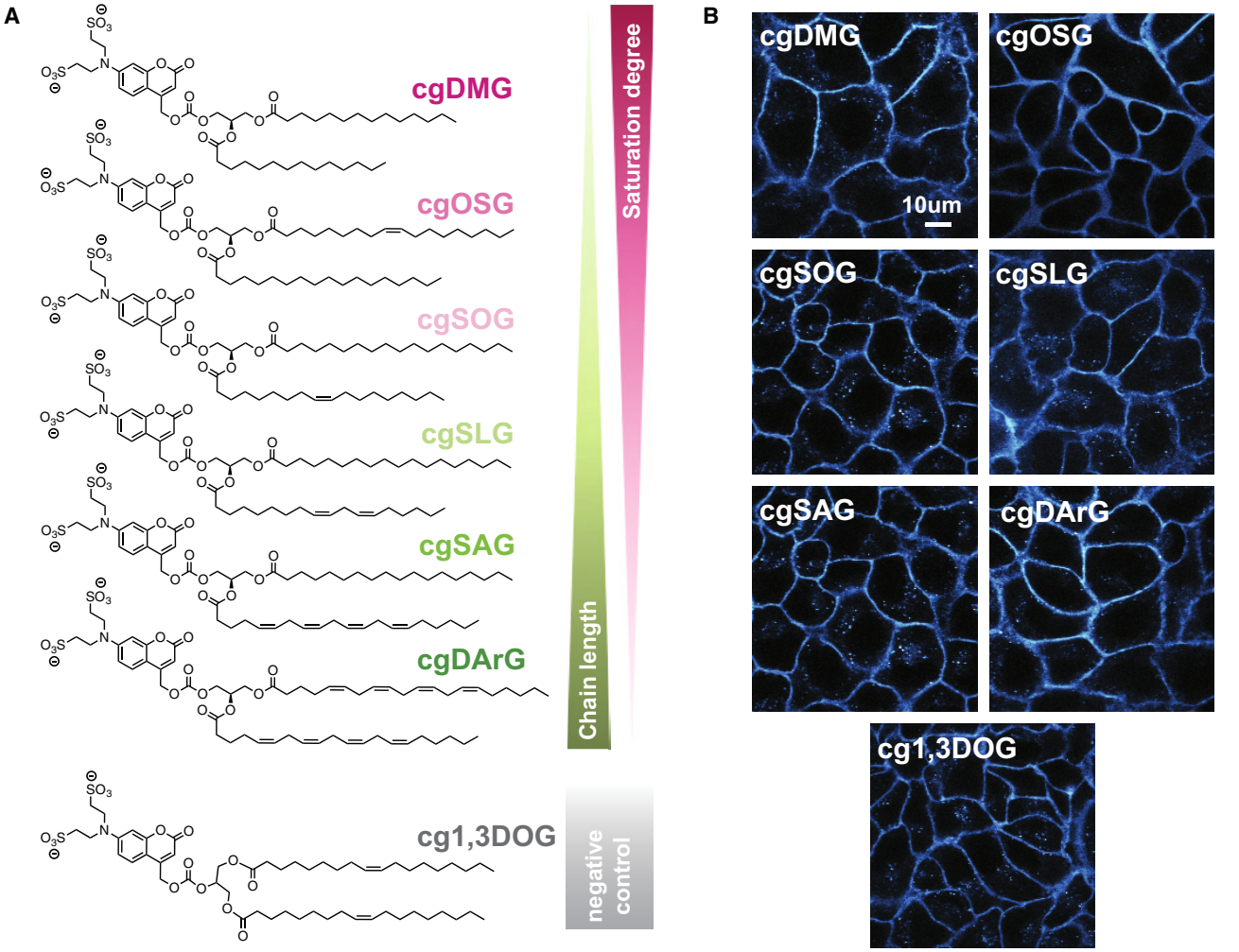

Figure 3. Chemistry of DAGs. (*A*) Chemical structures of the different DAGs used in this study sorted by increasing saturation degree (*top to bottom*). 1,3-Dioleoylglycerol does not recruit the C1-containing effector protein and is used as a negative control. (*B*) Confocal fluorescence microscopy of HeLa Kyoto cells with cgDAGs localizing in the plasma membrane. To see this figure in color, go online. (original)

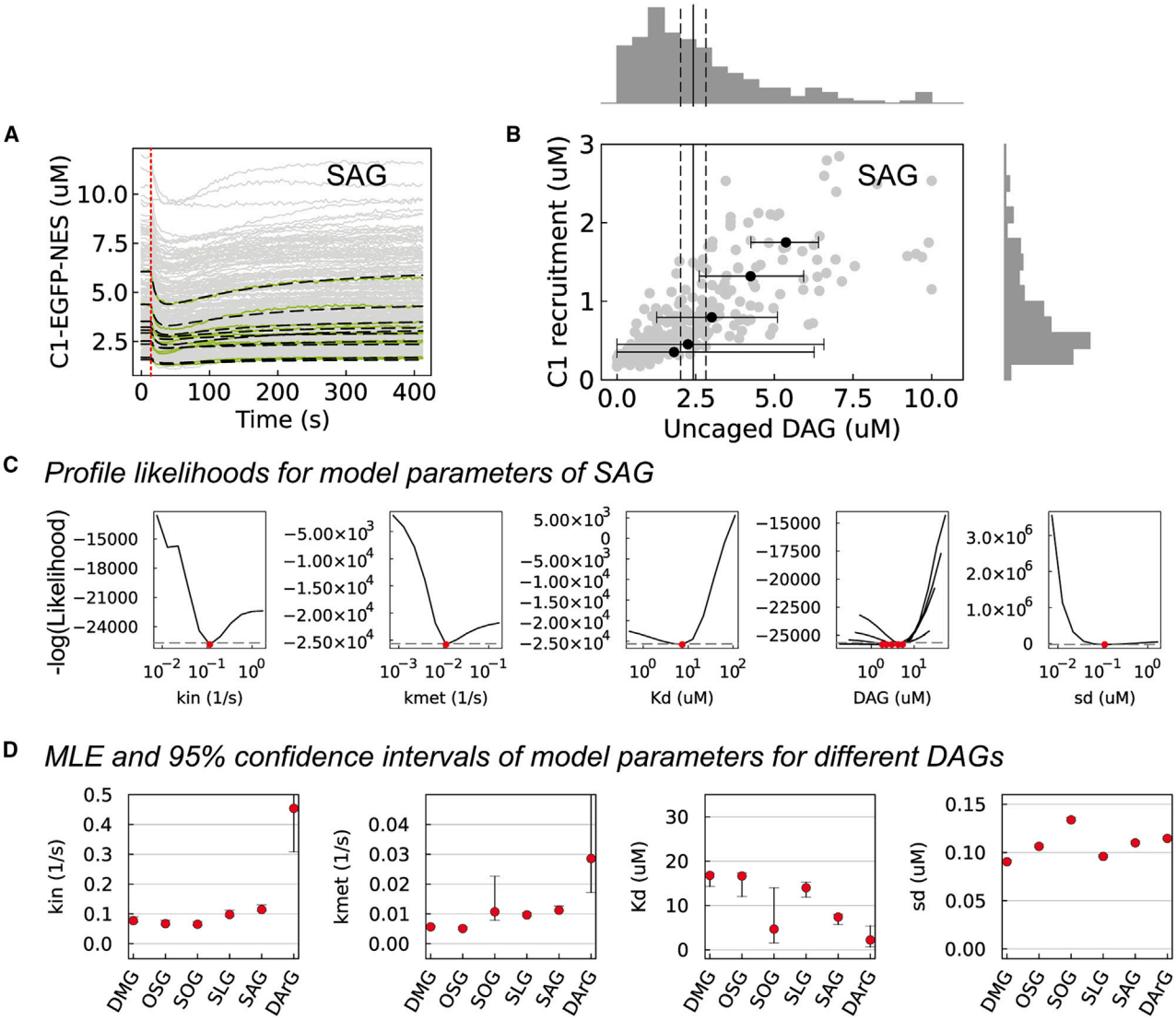

Figure 5. Fitting and parameter inference on single-cell experimental data. (*A*) Single-cell traces of C1-EGFP-NES dynamics (*gray lines*) after uncaging of SAG. Ten representative cell traces (*green lines*) and their respective fits (*dashed black lines*) are shown. Red vertical dotted line indicates the time of ultraviolet exposure that results in SAG uncaging. (*B*) Correlation between inferred uncaged SAG and measured C1-EGFP-NES recruitment in the cell population. Each gray dot refers to a single cell. Black dots with error bars show five representative cells and their 95% likelihood-based confidence intervals. Vertical solid and dashed lines indicate the experimentally measured mean and standard deviation of uncaged SAG. Marginal histograms of uncaged SAG and C1-EGFP-NES recruitment are shown on each axis. (*C*) Profile likelihoods of the model parameters. Gray horizontal dashed lines indicate the 95% likelihood-based confidence interval threshold, and red circles indicate the fit maximum likelihood estimation of the parameter. Profile likelihoods of uncaged SAG are shown for the same five representative cells as in (*B*). (*D*) Inferred model parameters and 95% likelihood-based confidence intervals of the different DAG lipid species. To see this figure in color, go online. (corrected)

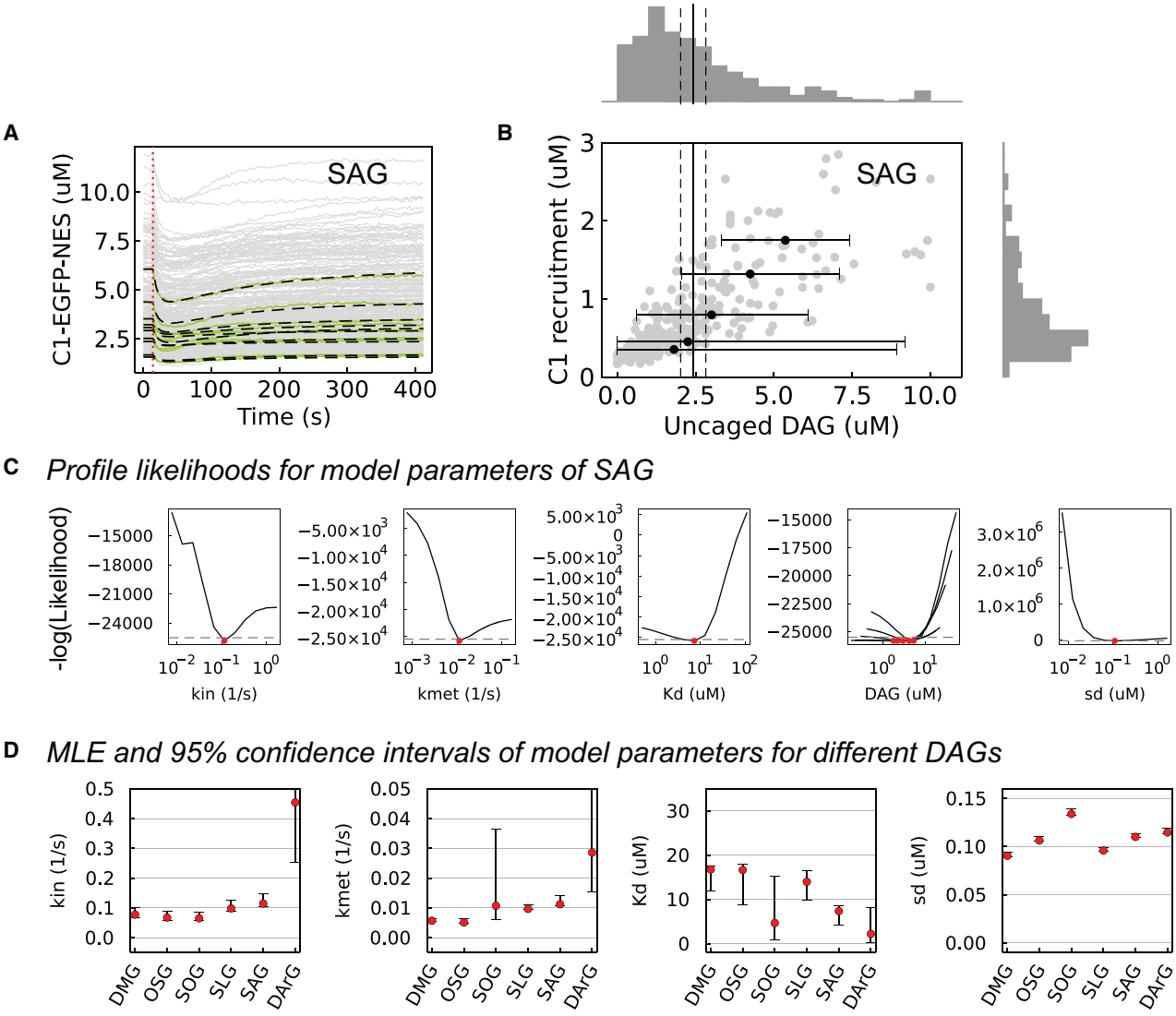

Figure 5. Fitting and parameter inference on single-cell experimental data. (*A*) Single-cell traces of C1-EGFP-NES dynamics (*gray lines*) after uncaging of SAG. Ten representative cell traces (*green lines*) and their respective fits (*dashed black lines*) are shown. Red vertical dotted line indicates the time of ultraviolet exposure that results in SAG uncaging. (*B*) Correlation between inferred uncaged SAG and measured C1-EGFP-NES recruitment in the cell population. Each gray dot refers to a single cell. Black dots with error bars show five representative cells and their 95% likelihood-based confidence intervals. Vertical solid and dashed lines indicate the experimentally measured mean and standard deviation of uncaged SAG. Marginal histograms of uncaged SAG and C1-EGFP-NES recruitment are shown on each axis. (*C*) Profile likelihoods of the model parameters. Gray horizontal dashed lines indicate the 95% likelihood-based confidence interval threshold, and red circles indicate the fit maximum likelihood estimation of the parameter. Profile likelihoods of uncaged SAG are shown for the same five representative cells as in (*B*). (*D*) Inferred model parameters and 95% likelihood-based confidence intervals of the different DAG lipid species. To see this figure in color, go online. (original)

SUPPORTING MATERIAL

Supporting material can be found online at https://doi.org/10.1016/j.bpj.2024.03.031.